Light Metals 2014
Edited by: John Grandfield
TMS (The Minerals, Metals & Materials Society), 2014

EFFECT OF THE THERMO-MECHANICAL TREATMENT ON IGC SUSCEPTIBILITY OF AA 5083 ALLOY

Tamara Radetić, Akram Halap, Miljana Popović and Endre Romhanji
Dept. of Metall. Eng., Faculty of Technology and Metallurgy, University of Belgrade; Karnegijeva 4; 11 120 Belgrade, Serbia

Keywords: Al-Mg alloys, Intergranular corrosion, Thermo-mechanical treatment

Abstract

This work reports on the effect of thermo-mechanical treatment on IGC susceptibility of the AA 5083 alloy. Specimens underwent varied amount of cold work and final annealing was conducted at 240°C. Extent of the cold work affected the IGC susceptibility of the alloy significantly. Microstructure characterization showed that depending on the amount of the cold work different deformation substructure was created, which, in turn, influenced morphology of precipitated β-phase (Al_3Mg_2). Formation of continuous film of the β-phase at the grain boundaries was observed in the specimens that were subjected to lower degree of the cold work and which were IGC susceptible. Better corrosion resistance characterized the specimens that underwent higher degree of the cold work (over 30-40%) due to β-phase precipitation in the form of discrete particles at the grain boundaries and in grain interiors.

Introduction

Aluminum alloy AA 5083 is characterized by good combination of properties such as good formability at moderate strength, weldability and corrosion resistance in atmospheric conditions [1]. However, the alloy has high Mg content (4.0-4.9 wt%) that makes it prone toward intergranular corrosion (IGC) and stress corrosion cracking (SCC) in certain environments due to the precipitation of anodic β-phase (Al_3Mg_2). Distribution and morphology of the β-phase precipitated during sensitisation treatment (annealing in 65-200°C temperature range) was subject of the numerous recent studies [2-11]. Although, the β phase forms heterogeneously at grain boundaries and preexisting primary particles, only the grain boundary precipitation contributes to increased IGC [2, 5]. Formation of the continuous film of the β-phase is detrimental for the corrosion resistance of the alloy. There are reports that extent of precipitation and susceptibility of the boundary toward IGC is related to the grain boundary character [4]. Grain morphology and distribution of the grain boundary types in polycrystalline material could be controlled by thermo-mechanical treatment. However, only a few studies [12-15] were directed on the effect of thermo-mechanical processing on the precipitation of the β-phase and corrosion properties. In this paper, we report on the effect of cold work on the β-phase precipitation during subsequent annealing and resulting susceptibility toward the IGC.

Experimental Procedure

The alloy used in this study was industrially hot rolled 7.4 mm thick plate supplied by Impol-Seval Rolling Mill, Serbia.

Table I Chemical compositions of the studied and standard AA5083 alloys

	Mg	Mn	Cu	Fe	Si	Zn	Cr	Ti	Sr
Study	5.13	.72	.13	.34	.11	.51	.008	.025	.003
5083	4.0 - 4.9	.4 - 1.0	< 0.1	< .4	< .4	< .25	.05 - .25	< .15	< .005

Composition of the alloy was close to aluminum AA5083 alloy with Mg and Zn contents somewhat higher than in the standard alloy (Table I).

The as-received alloy plate was further processed in the laboratory conditions. Thermo-mechanical treatment of the plate involved cold rolling to the plate thickness of 3.5mm, annealing at 350°C for 3h that was followed by cold rolling with various thickness reductions in the range 15-50%. Cold rolled specimens were finally annealed for 2h at 240°C.

In order to evaluate the effect of cold work, i.e. different thickness reductions, on the susceptibility to IGC of the alloy, Nitric Acid Mass Loss Test (NAMLT) following the ASTM G67 standard [16] was performed. Specimens, with dimensions 50 x 6 mm, were immersed into concentrated HNO_3 at 30°C for 24h, and the mass loss was measured. At least 3 specimens were tested for each state. For selected states, additional specimens were immersed in concentrated HNO_3 at 30°C for various times (2, 6, 24h) and their surface morphologies were characterized in the scanning electron microscope (SEM - JEOL JSM-6610LV at 20 kV).

Specimens for the TEM characterization were prepared by mechanical thinning, dimple grinding and ion milling. Ion milling was conducted at 5keV and incidence angle of 5° till perforation while further cleaning was done at 1 and 0.5keV. Specimen holder was cooled by liquid nitrogen to avoid any overheating during the ion-milling. Specimens were characterized in JEOL 100 CX microscope.

Electrical conductivity measurements were performed on Foerster Sigmatest 2.069 instrument at the operating frequency of f = 120kHz. Electrical resistivity was calculated as reciprocal value of the conductivity.

Experimental Results and Discussion

Variation of the IGC susceptibility (expressed as a mass loss in the NAMLT test) as a function of the thickness reduction is shown in Figure 1.

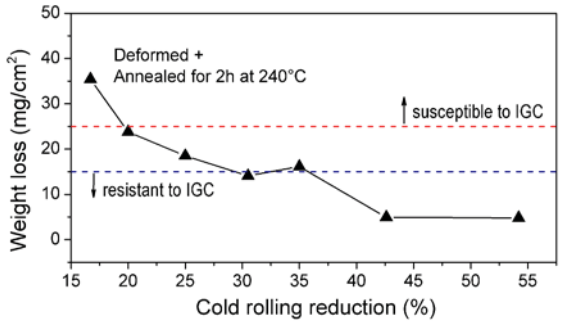

Figure 1 Intergranular corrosion (IGC) susceptibility determined by NAMTL test [16] as a function of the thickness reduction.

The results of the NAMLT test show that an increase in the thickness reduction, i.e. in the amount of the cold work, reduces IGC susceptibility of the alloy. The IGC resistant states were achieved at deformations higher than 35%. After reaching a certain level of the deformation, around 40%, further reductions did not alter IGC susceptibility of the alloy. These results show that, even if the final annealing conditions were the same, varied amounts of the cold work gave rise to IGC susceptible as well as IGC resistant states. Surfaces of the IGS susceptible (16% deformation) and IGC resistant (42% deformation) specimens after exposure to the nitric acid had distinct morphologies indicating different mechanisms of the corrosion attack.

Typical surfaces of the specimens deformed 16% (IGC susceptible) after immersion into the nitric acid for various times are shown in Figures 2 and 3. After the immersion for 2h, corrosion of the surface corresponding to LT plane was non-uniform (Figure 2). Unbinding and fall out of grains was observed in the corroded areas. The attack of the acid was localized at the grain boundaries whereas the grain interiors appeared unaffected. In the areas in which flat surface layer had not been completely removed, polygonal grains were outlined by preferentially attacked grain boundaries (Figure 2a). Similar, non-uniform corrosion spreading of sensitized AA 5083 exposed to different corrosive environment, NaCl solution, was reported by Jain et al [17].

Extending the immersion time resulted in spreading of the corrosion throughout the surface. No remains of the flat surface layer were observed after the 24h in acid and multiple layers of grains got unbound and fell out (Figure 2b). Even after extended exposure to the corrosive environment, grain's surfaces stayed intact - smooth and faceted (Figure 3a). Flat facets point out on wetting of the boundaries by the film of the β-phase. Corrosion mechanism appears to be severe corrosion and dissolution of the β-phase that resulted in the unbinding of grains and caused large mass loss in this state.

In contrast, in the specimens that underwent 42% thickness reduction (IGC resistant), both grain boundaries and grain interiors were corroded after the immersion into the nitric acid (Figures 3b and 4). Elongated grains and irregular outlines of grain boundaries characterized morphology of the surfaces in LT orientation (Figure 4). Corrosion appeared to proceed layer by layer, and although more material was removed from the surface after 24h, no deepening and unbinding of the individual grains was observed. Net result was gradual removal of material and low mass loss. Rough, sponge like surface of the grains indicates that corrosion also took place in the grain interiors (Figure 3b).

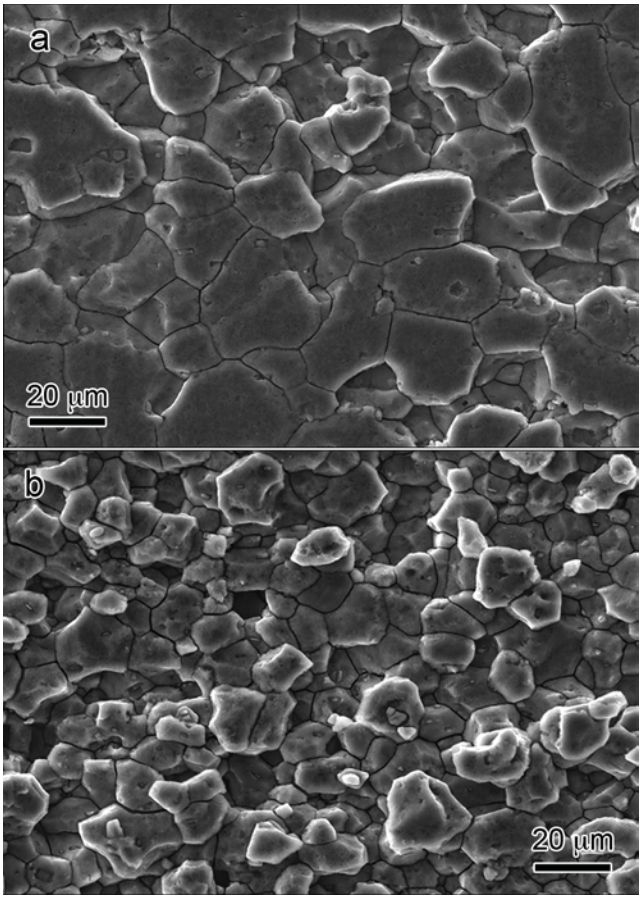

Figure 2 Secondary electron SEM micrographs showing morphology of the surface parallel to LT plane. Specimens were deformed 16% and annealed for 2h at 240°C (IGC susceptible). Specimens were immersed in the nitric acid for: (a) 2h - Below surface layer of flat grains, polygonal grains emerge due to the grain fall out. (b) 24h - Polygonal and faceted grains in multiple layers are observed as grains got unbound and fall out.

Unaffected grain interiors, corrosion confined to the grain boundaries that results in grain fall out appear to be the signature of the IGC susceptible states while corrosion of both grain boundaries and grain interiors is characteristic of IGC resistant states in AA5083 and other Al-Mg alloys since similar morphological features were also observed in the 5083 alloy that underwent different thermo-mechanical regimes [13]. In general, cause of corrosion in Al-Mg alloys is a large difference between corrosion potential of anodic β-phase and Al-matrix. Corrosion of the grain boundaries as well as the grain interiors in IGC resistant specimens indicates lower potential difference between them, than in the case of IGC susceptible state in which grain boundaries were solely attacked. According to some early models [2], precipitation within grains actually decreased potential difference between the matrix and anodic grain boundaries covered with the β-phase, decreasing the driving force for the preferential corrosion/ attack on the grain boundaries.

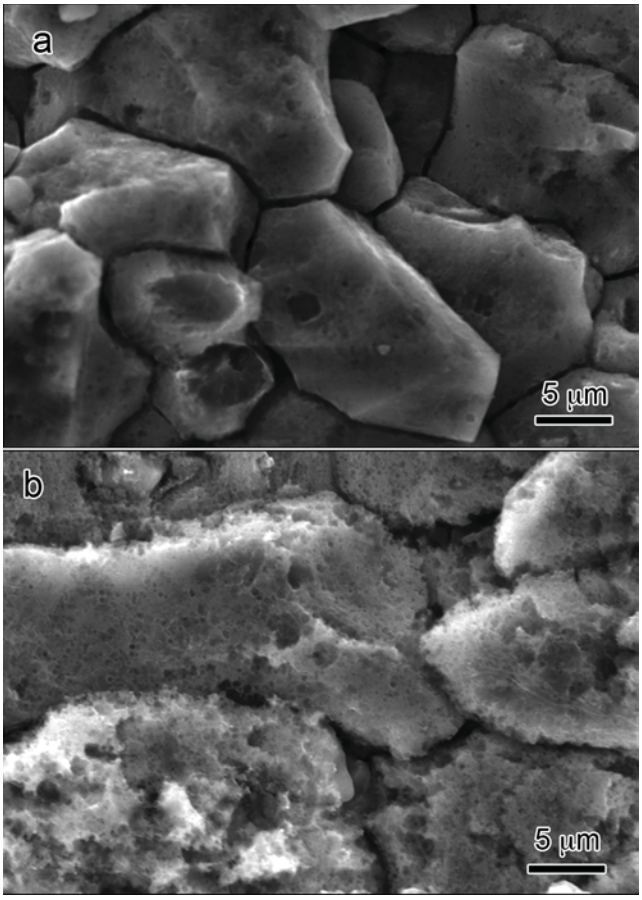

Figure 3 Secondary electron SEM micrographs of the surface morphology at higher magnifications: a) Specimen deformed 16 % and annealed for 2h at 240°C (IGC susceptible) after immersion 24h in the nitric acid. Dissolution of the corroded β-phase left behind channels that separate distinct, individual grains. Grains' surfaces are smooth and faceted. b) Specimen deformed 42% and annealed for 2h at 240°C (IGC resistant) after immersion 24h in the nitric acid. Both grain boundaries and grain interiors were corroded.

In the specimens deformed 16% (IGC susceptible), extent of the corrosion diminished from the edge toward the central part of the cross-section at the surface corresponding to the LS plane, after 2h in the acid (Figures 5a and b). In the region close to the edge (Figure 5a), the response was same as one observed at the surface corresponding to the LT plane. Grains were polygonal, and grain fall out occurred in the corroded areas. In the central part, corrosion and removal of the flat surface layer was very limited. Grains were coarser, elongated and more irregular in shape.

Longer immersion in the acid lead to corrosion of the whole surface, but the difference in the surface morphology along the cross-section persisted. While surfaces of the grains close to the edge stayed smooth and faceted and mechanism of the mass loss was grain unbinding and fall out, in the central region, grain interiors were also attacked. Irregular, corroded surface of the grains were observed (Figure 5c).

In the specimen deformed 42% (IGC resistant state), corrosion was uniform throughout the cross-section and surface morphology did not change significantly from 2h to 24h (Figure 6). Exfoliation of thin, fibrous grains, with attacked both grain boundaries and grain interiors, was observed.

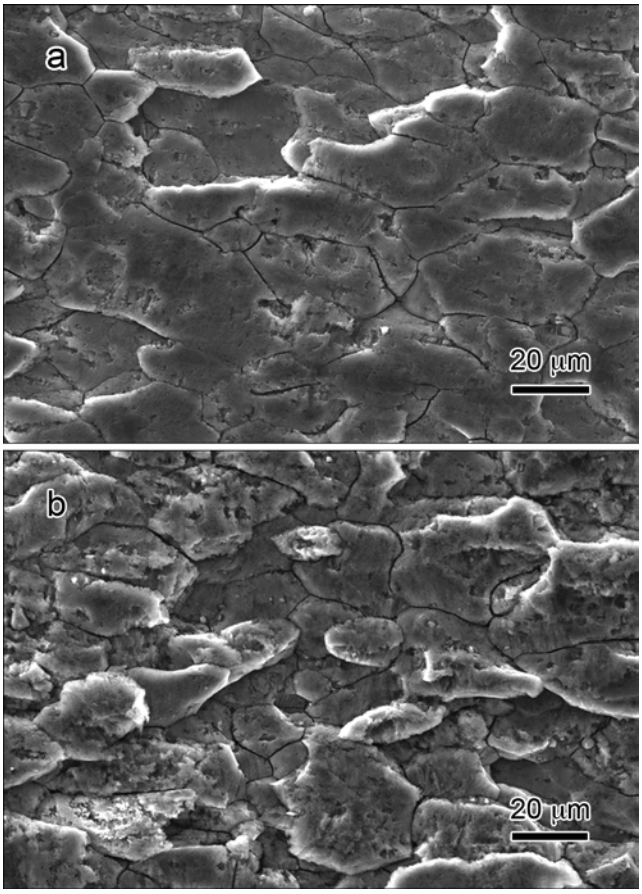

Figure 4 Secondary electron micrographs showing morphology of the surface parallel to LT plane. Specimens were deformed for 42% and annealed for 2h at 240°C (IGC resistant). Specimens were immersed in the nitric acid for: (a) 2h - Below surface layer of flat grains, another layer of elongated, irregular grains is observed. (b) 24h - Corrosion appears to proceed layer by layer.

Differences in uniformity of the corrosion attack are related to the extent of the cold work and uniformity of deformation within plates. At low reduction such as 16% (IGC susceptible state), deformation is not homogenous throughout the plate thickness. Close to the surface, the material was more deformed what after recovery resulted in polygonal, faceted grains that are prone toward fall out and IGC. Toward the center, microstructure was less affected by the deformation, advancement of the recovery was lower, resulting in irregular grain substructure and, interestingly, response toward the nitric acid became similar to one observed in IGC resistant state.

Grain substructure introduced by the different amount of the cold work and subsequent precipitation of the β-phase determined propensity of the alloy toward IGC. TEM characterization showed that in the case of the of 16 % deformation (IGC susceptible state) continual or semi-continual film of the β-phase covered grain boundaries (Figure 7a). In the specimen deformed 42% (IGC resistant state), discrete, lenticular precipitates were observed (Figure 7b).

Morphology of the β-phase is determined by the deformation substructure and nature of the grain boundaries that formed during plastic deformation and subsequent recovery. Substructure developed at higher deformation consisted of microbands that during the annealing recover into the extensive network of cells and subgrains (Figure 7c). Irregular morphology of the grain boundaries implying frequent change in their character is one of the characteristics of the IGC resistant states. Grain boundary crystallography is one of the factors that control precipitation of the β-phase according to the findings of Davenport et al. [4]. Hence, despite the large fraction of interfaces in the specimens, precipitation of the β-phase occurred almost exclusively at the triple junctions and high angle grain boundaries while subgrain boundaries were precipitates free. At lower reductions that result in IGC susceptible states, long and straight grain boundaries were observed. Wetting of such boundaries by the β-phase made them IGC susceptible. Those observations point out that higher deformation creates substructure that favors precipitation of the β phase as discrete particles. Since only certain grain boundary types have the propensity to be wetted by the β-phase, variability of the boundary type does not allow for the formation of extended patches of the film.

That the morphology of the β-phase has a key role in determining the IGC susceptibility of the alloy is further supported by electrical resistivity measurements. By following changes in the electrical resistivity of the processed specimens, it was possible to evaluate microstructure changes, such as precipitation or dissolution, occurring in the alloy [18]. In this particular case, electrical resistivity decrease is related to the precipitation of the β-phase [19]. Results showed larger resistivity drop for the IGC resistant states (Figure 8), indicating that the larger amount of the β-phase precipitated in those states. Such observation, together with microstructural characterization, leads to the conclusion that IGC susceptibility in the great extent depends on morphology and distribution of the β-phase and not so much on the amount of precipitation.

Summary

This study showed that the amount of the cold work has a significant effect on the IGC susceptibility of the alloy. Varied amounts of the cold work can create such grain substructure that favors precipitation of the continuous film of the β-phase at the grain boundaries and results in the IGC susceptible state as well as substructure in which discrete precipitation of the β-phase occurs leading to the IGC resistant material.

Characterization of the surfaces of the alloy exposed to the nitric acid showed that in IGC susceptible material corrosion was localized at the grain boundaries wetted by the β-phase while Al-matrix grain's interiors were intact. In the IGC resistant material, corrosion attack was uniform – both grain interiors and grain boundaries were corroded, however, overall mass loss was low.

Acknowledgement
This research was supported by Ministry of Education, Science and Technological Development, Republic of Serbia, and Impol-Seval Aluminum Mill, Sevojno, under contract grant TR 34018.

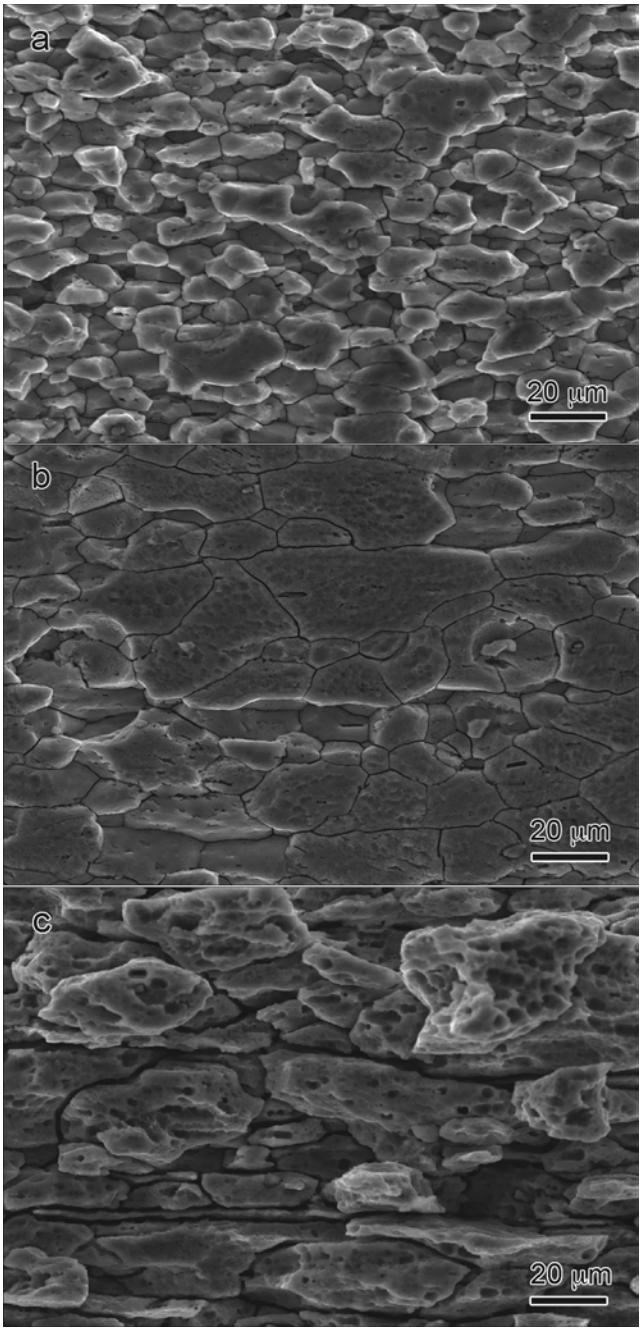

Figure 5 Secondary electron micrographs of morphology of the surface parallel to LS plane. Specimens were deformed for 16% and annealed for 2h at 240°C (IGC susceptible) that were immersed in the nitric acid. Corrosion is greater close to the edges than in the central part. (a) In the edge region after 2h in acid, multilayers of polygonal grains are visible in addition to the remaining surface layer. (b) In the central region, after 2h in the acid, corrosion extent is very limited. Most of the surface layer is preserved and preferentially attacked grain boundaries delineate elongated grains. (c) After 24h in the acid, the central region underwent corrosion both grain boundaries and grain interiors.

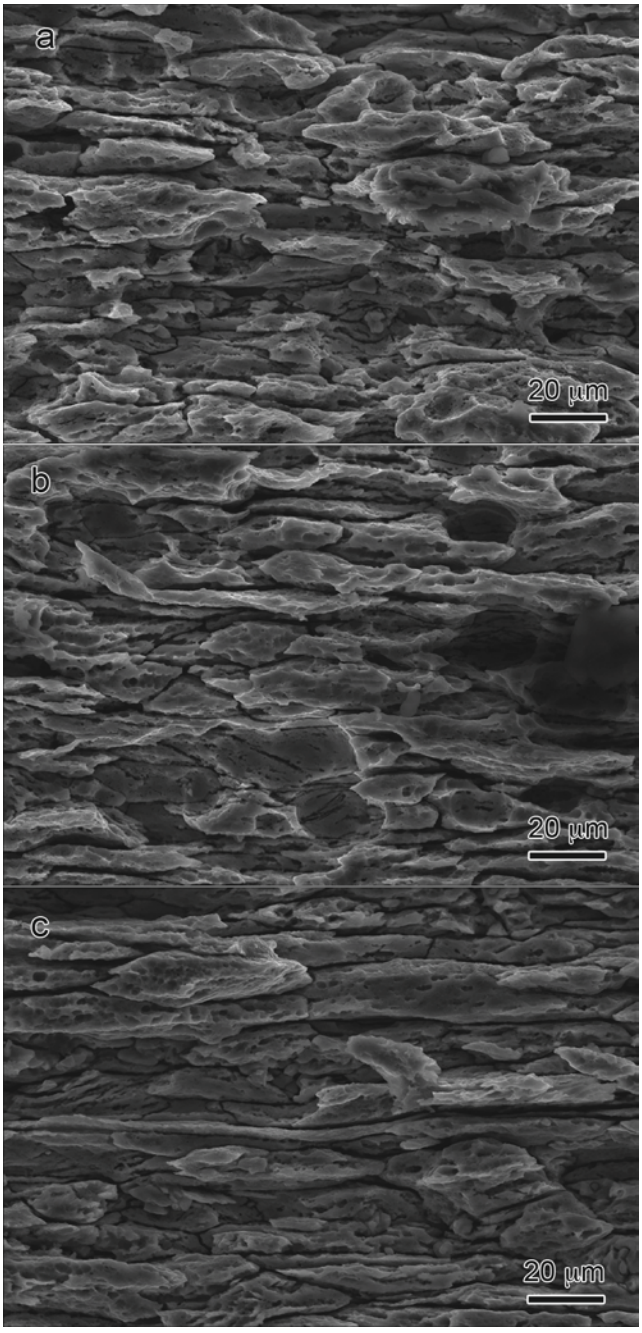

Figure 6 Secondary electron micrographs of morphology of the surface parallel to LS plane. Specimens were deformed for 42% and annealed for 2h at 240°C (IGC resistant) that were submerged in the nitric acid: (a) In the edge region after 2h in acid, exfoliation of the fibrous grains was observed. (b) In the central region, after 2h in the acid, surface morphology has same features as in the edge region. (c) Surface morphology after 24h in the acid.

Figure 7 Bright Field TEM micrographs of the precipitated β-phase at the grain boundaries: (a) Specimen deformed 16% and annealed 2h at 240°C (IGC susceptible). (b) Specimen deformed 42% and annealed 2h at 240°C (IGC resistant). (c) Cell substructure in the specimen deformed 42% and annealed 2h at 240°C (IGC resistant). Arrows indicate β-phase precipitates.

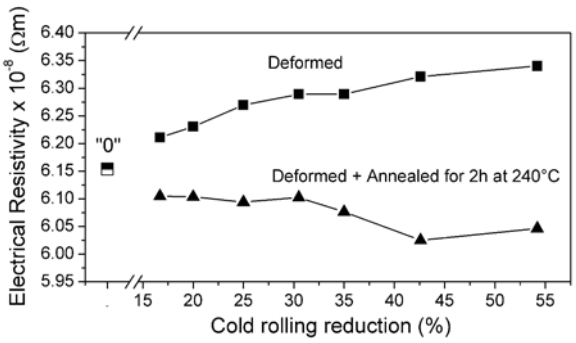

Figure 8 Electrical resistivity as a function of thickness reduction. All specimens were annealed 2h at 240°C. Electrical resistivity of the referent state corresponding to specimens that underwent initial cold rolling and intermediate annealing of 3h at 350°C is marked as "0".

References

1. Dietrich G. Altenpohl, *ALUMINUM: Technology, Applications and Environment* (6th ed., The Aluminum Association, Washington D.C., and TMS, Warrendale, Pennsylvania, 1999), 349.
2. J.L. Searles, P.I. Gouma and R.G. Buchheit, "Stress Corrosion Cracking of Sensitized AA5083," *Metallurgical and Materials Transactions A*, 32A (2001), 2859-2867.
3. R.H. Jones, D.R. Baer, M.J. Danielson and J.S. Vetrano, "Role of Mg in the Stress Corrosion Cracking of an Al-Mg Alloy," *Metallurgical and Materials Transactions A,* 32A (2001), 1699-1711.
4. A.J. Davenport et al., "Intergranular Corrosion and Stress Corrosion Cracking of Sensitized AA5182," *Materials Science Forum*, 519-521 (2006), 641-646.
5. R. Goswami et al., "Precipitation behavior of the β phase in Al-5083," *Materials Science and Engineering A*, 527A (2010), 1089-1095.
6. R. Goswami, et al, "Microstructural Evolution and Stress Corrosion Cracking Behavior of 5083," *Metallurgical and Materials Transactions A*, 42A (2010), 348-355.
7. J. Gao and D.J. Quesnel, "Enhancement of the Stress Corrosion Sensitivity of AA5083 by Heat Treatment" *Metallurgical and Materials Transactions A*, 42A (2010), 356-364.
8. R.L. Holtz et al., "Corrosion Fatigue Behavior of Aluminum Alloy 5083-H131 sensitized at 448 K (175°C)," *Metallurgical and Materials Transactions A*, 43A (2011), 2839-2849.
9. N. Bernstein, R. Goswami, and R.L. Holtz, "Surface and Interface Energies of Complex Crystal Structure Aluminum Magnesium Alloys," *Metallurgical and Materials Transactions*, 43A (2012), 2166-2176.
10. Y. Zhu et al., "Evaluation of Al_3Mg_2 Precipitates and Mn-rich phase in Aluminum-Magnesium Alloy Based on Scanning Transmission Electron Microscopy Imaging," *Metallurgical and Materials Transactions A*, 43A (2012), 4933-4939.
11. M. Popović, T. Radetić, and E. Romhanji, "Precipitation of the β-phase and Corrosion Behavior of an Al-6.8wt.%Mg Alloy," in *ICAA13: 13th International Conference on Aluminum Alloys*, ed. H. Welland, A.D. Rollett and W.A. Cassada, (John Wiley & Sons, Inc., Hoboken, NJ, USA, 2012), 363–368.
12. J.C. Chang and T.H. Chuang, "Stress Corrosion Cracking Susceptibility of the Superplastically Formed 5083 Aluminum Alloy in 3.5 Pct NaCl Solution," *Metallurgical and Materials Transactions A*, 30A (1999), 3191-3199.
13. J.C. Chang and T.H. Chuang, "The Degradation of Corrosion Resistance for Al 5083 Alloy after Thermal and Superplastic Forming Processes," *Journal of Materials Engineering and Performance*, 9 (2000), 253-260.
14. L. Tan and T.R. Allen, "Effect of Thermomechanical Treatment on the corrosion of AA5083," *Corrosion Science*, 52 (2010), 548-554.
15. G.R. Argade, N. Kumar and R.S. Mishra, "Stress Corrosion Cracking Susceptibility of Ultrafine grained Al-Mg-Sc Alloy," *Materials Science and Engineering A*, 565A (2013), 80-89.
16. ASTM G67-04: Standard test method for determining the susceptibility to intergranular corrosion of 5xxx series aluminum alloys by mass loss after exposure to nitric acid (NAMLT test), ASTM International, West Conshohocken, PA, 2004.
17. S. Jain et al., "Spreading of Intergranular Corrosion on the Surface of Sensitized Al-4.4Mg Alloys: A general Finding," *Corrosion Science*, 59 (2012) 136-147.
18. S.I. Vooijs et al., "Monitoring the Precipitation Reactions in a Cold-Rolled Al-Mg-Mn-Cu Alloy Using Thermoelectric Power and Electrical Resistivity Measurements," *Philosophical Magazine A*, 81A (2001), 2059-2072.
19. M. Popović and E. Romhanji, "Characterization of Microstructural Changes in an Al-6.8wt%Mg Alloy by Electrical Resistivity Measurements," *Materials Science and Engineering A*, 492A (2008), 460-467.